Technical Assessment of Dye-Sensitized Solar Cell Building Integrated Photovoltaics in Office Buildings

Zoltan Varga[1, 2, 3,*], Ervin Racz[3], Marek Bobcek[4] and Zsolt Conka[3,4]

[1]Doctoral School of Applied Informatics and Applied Mathematics, Obuda University, Bécsi út 96/b, H-1034 Budapest, Hungary; varga.zoltan@uni-obuda.hu

[2]John von Neumann Faculty of Informatics, Obuda University, Bécsi út 96/b, H-1034 Budapest, Hungary

[3]Kandó Kálmán Faculty of Electrical Engineering, Obuda University, Bécsi út 96/b, H-1034 Budapest, Hungary, racz@uni-obuda.hu; conka.zsolt@kvk.uni-obuda.hu

[4]Technical University of Kosice, Letná, 1/9, 04001 Kosice, Slovakia, marek.bobcek@tuke.sk; zsolt.conka@tuke.sk

* Corresponding author

Abstract: Building Integrated Photovoltaic (BIPV) systems play an important role in the mitigation of carbon dioxide emissions in cities. Furthermore, Dye Sensitized Solar Cell (DSSC) is an attractive technology, with its' uniform and semitransparent appearance. Concerning this, the current study helps engineers and architects in decision-making concerning the integration of DSSC modules, for suitable building designs. The aim of the study is to develop and validate an integrated simulation framework that allows a detailed assessment of the performance of the BIPV DSSC system under urban conditions. For these purposes, the building's energy consumption, electrical energy generated by the BIPV DSSC system, and energy price scenarios have been simulated. Nevertheless, optimization techniques have been applied for further investigations. Based on the results, it can be concluded that Dye-Sensitized Solar Cell offer a significant promise for BIPV systems, but the performance of the module is seasonal and might not guarantee enough energy coverage for the building's consumption. Nevertheless, applying linear programming approaches revealed that there are electricity price scenarios, that enable the BIPV DSSC system to become feasible.

Keywords: Dye-Sensitized Solar Cell; DSSC; Building Integrated Photovoltaic System; BIPV; SARIMAX; Simulation; Optimization; Linear Programming

1 Introduction

Greenhouse gas emissions have been growing rapidly due to our way of electricity generation. Energy generation relies heavily on fossil-based fuels; however, renewable energy sources play an important role in electricity generation. Based on some prognostications, renewable energy sources are expected to exceed the dominant role of coal by 2030 [1]. Conversely, renewable energy sources help to mitigate environmental issues (i.e., high concentration of carbon dioxide (CO_2) in the atmosphere) [2] [3]. Amongst the renewable energy sources, photovoltaic (PV) has received a great deal of attention, and it converts a portion of the incoming solar power into electricity. PV has gained significant ground in architecture because it can be merged with architectural structures, notably efficiently resulting in Building-Integrated Photovoltaic (BIPV) [4] [5]. This technology offers a great deal of benefits, including increased energy independence, improved sustainability, and reduced energy cost [6]. Furthermore, these systems serve as a functional component of the building's design. Moreover, the energy consumption of buildings in megacities (e.g. Tokyo, Hong Kong, New York) is much higher than the energy consumption in transport sectors, resulting in huge CO_2 emissions [7]. Therefore, BIPV technology can reduce the CO_2 emissions and supply the building's own demand and use the energy directly without transmission fees.

Among PVs, silicon-based technologies share a dominant role (about 90%) in the market. Mostly, these PV technologies fall into standard in-roof system type classification, and BIPV represents only 1% of the global PV market [8]. The initial development of the new generation PV modules involves transparency, resulting in the integration of buildings. The advantages of the semi-transparent third-generation photovoltaic systems are (i) they can generate electricity in diffuse light; and (ii) have architectural visibility with uniform appearance, making them attractive in cities [9]. Dye-Sensitized Solar Cell (DSSC) is a third-generation device that benefits from the low-cost and ease of manufacturing compared to traditional silicon-based devices because the manufacturing materials do not require complex fabrication techniques. The conventional DSSC consists of five essential components which are (i) glass substrate with transparent conductive oxide; (ii) a wide band-gap semiconductor layer, usually titanium-dioxide; (iii) sensitizing dye that attached to the surface of the semiconductor layer; (iv) electrolyte solution containing iodide and triiodide ions; (v) counter electrode [10]. Attention should be drawn to the fact that the combination of materials and manufacturing temperature in the fabrication of the DSSC has a significant role, especially in long-term efficiency. Beyond that, particle connectivity and crystallinity of the semiconductor layer are improved via the sintering processes. On the other hand, high heat can damage the device and can lead to mechanical stress and degradation. Factors such as module temperature, shadowing, orientation, and angle must be taken into consideration before the final construction to make the BIPV system work effectively. Because of the unique properties of the DSSC device, BIPV DSSC has

a great opportunity to optimize the electricity generation of buildings. Roy et al. made color comfort analysis for two years in exposed DSSC. It was concluded that the enhanced color properties make it a potential candidate for low-energy building integration [11]. Shukla et al. reviewed the opportunities and challenges of the BIPV in Southeast Asian countries. The possible design and integration strategies are identified in their article, including vertical curtain wall, stepped curtain wall, atrium space, and multifunctional applications (such as noise reduction) [12].

According to Scopus research, 106 relevant publications were identified focusing on the application of DSSC as a BIPV system. It was revealed that the majority of the work focuses on material characterization, whereas real-world case studies and review papers are limited. Moreover, the majority of studies on material characterization are experimental work, and controlled laboratory settings were used, while case study type of work incorporated simulation and experimental techniques. Corrao et al. investigated the optical performance of the DSSC integrated glass block. Solar factors, the light transmittance, and the shading coefficient of the device have been simulated numerically. The simulation study explores how the placement of DSSCs on the surface of the glass block can influence energy absorption. Moreover, placing it on the external surface of the block results in about 10% higher energy absorption than in the case of internal placement [13]. Cornaro et al. investigated the thermal and electrical characterization of a DSSC module, a double junction amorphous silicon device, and a multi-crystalline silicon device under outdoor operating conditions. The outdoor tests were monitored and lasted for 3 months, which included continuous data collection. Based on their findings, DSSC demonstrated lower temperature sensitivity and higher energy generation during non-peak sunlight hours, such as morning and afternoon hours [14]. Hyun et al. analyzed the DSSC BIPV in the case of an office building (OB) in various climate zones. Four climate tones in the United States had been taken into consideration for the analysis. Based on their simulation approach, it was found that the heating energy demand was reduced due to the insulation of DSSC windows, and the cooling energy demand was slightly increased [15]. Lund et al. investigated the long-term performance of 248 commercial 30 × 30 cm semi-transparent DSSC modules. Based on six years of monitoring, under real outdoor conditions in Denmark, they assessed the power output and chemical stability. It was shown that 88-90% efficiency losses occurred in the south-facing modules over the six years, whereas modules facing north obtained their original efficiency [16]. Kishore et al. explored the energy influence of office buildings, taking the effect of window-to-wall ratio (WWR) into account across five different U.S. climate zones. According to the research evaluation using simulation techniques, triple-glazed DSSC-integrated windows demonstrated a suitable choice for small buildings by enhancing energy efficiency [17]. Gholami et al. investigated how different climate conditions impact solar radiation components on BIPV materials. Stavanger in Norway, Bern in Switzerland, Rome in Italy and Dubai in the UAE, were selected for the investigation. It was revealed that the climate has a significant impact on DSSC technologies compared to mono-

Si, poly-Si, and Copper Indium Gallium Selenide (CIGS) technologies. Furthermore, DSSC maintains high efficiency under low and diffused light conditions (such as cloudy climates) [18]. Reale et al. evaluated the energy generation potential of DSSC BIPV applications. In addition, their study includes real outdoor experimental measurements for validation. The findings indicate that the DSSC module is suitable for vertical façade integration in BIPV systems, and it demonstrated outstanding performance under diffuse light conditions [19]. Other scientists also assessed the performance of the DSSC as BIPV by applying an experimental investigation [20]. Furthermore, studies related to the analysis of the performance of DSSC as BIPV in specific geographical locations and climate conditions have also been conducted [21].

According to the studied literature, the DSSC BIPV topic is a highly researched field with a great deal of publications involving experimental investigations and numerical simulations. Also, it can be concluded that the harvested electrical energy and thermal energy significantly cover a huge share of the building's energy consumption. Although this is an intensive research topic, to the best of our knowledge, there is no literature presenting the performance of the building-integrated DSSC in office buildings for an entire urban district. The motivation is to advance renewable and sustainable electricity generation in urban environments and to minimize environmental impacts. The main aim of the research is to evaluate the potential of DSSC as a BIPV system based on technical capabilities. In this regard to address the challenges, the current research objective is to apply simulation-based approaches to evaluate the following key scientific questions: (i) how much electrical energy can be generated if the facades of office buildings covered with DSSC modules taking the environment factors into account; (ii.i) is there an existing building facades combination for each building that satisfies the defined positive-minimum-value optimization criteria; (ii.ii) if no feasible solution has been found, which selling-to-buying electricity price scenario would be feasible for the optimization framework; (iii) what percentage of a building's electricity demand could be covered by DSSC BIPV system on the most suitable facades. With respect to this, the current study helps engineers and architects in decision-making concerning the integration of DSSC modules into suitable building designs. The expansion of the BIPV DSSC systems in metropolitan areas could lead to decreased cell production costs.

2 Methods

2.1 Typology

To fulfill the aim of the research, the district exhibiting the greatest number of office buildings was selected for further investigation. Therefore, a comprehensive spatial analysis has been conducted to identify this district. Figure 1 shows the distribution of office buildings in Budapest using a heatmap representation, highlighting District 13 as it contained the highest number of OBs.

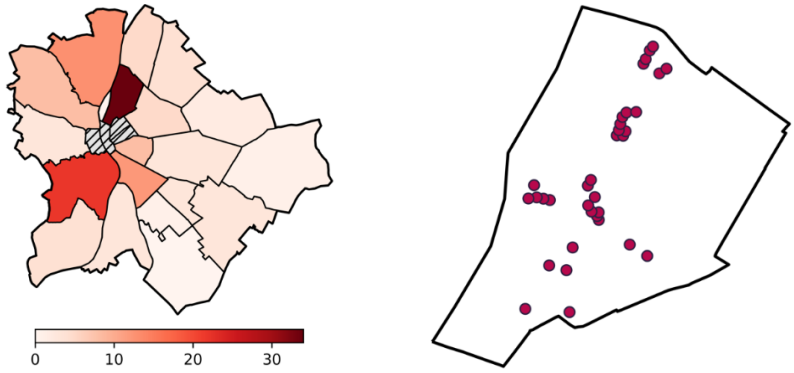

Figure 1
The distribution of office buildings in Budapest is shown using a heatmap representation. The left side map illustrates the density in each district in a heatmap, whereas the right-side image zooms into District 13, which contains the highest number of office buildings.

During the framework, the urban heat island (UHI) effect has been taken into account. UHI plays an important role in microclimatic conditions in urban environments. With respect to this, urban areas experience higher temperatures due to building materials, infrastructure density, and the surface area of green spaces is significantly smaller. In this context, the thermal performance and efficiency of the installed BIPV system were influenced, leading to reduced effectiveness and suboptimal electrical energy generation [22]. Consequently, districts in which UHI occurred were left out of the assessment.

2.2 Simulation Approach

The applied simulation approach is presented using a flowchart diagram in which the steps of the simulation process are outlined. Figure 2 shows the flowchart diagram of the present work where five main sequences of operations are illustrated: (i) simulation of electrical energy generated by BIPV DSSC modules (highlighted in yellow); (ii) simulation of OB electrical energy consumption (represented in green); (iii) electricity price determination (marked in blue); (iv) generating GeoJSON files for visual representation (depicted in gray); and (v) solving optimization problem using combination techniques (highlighted in red).

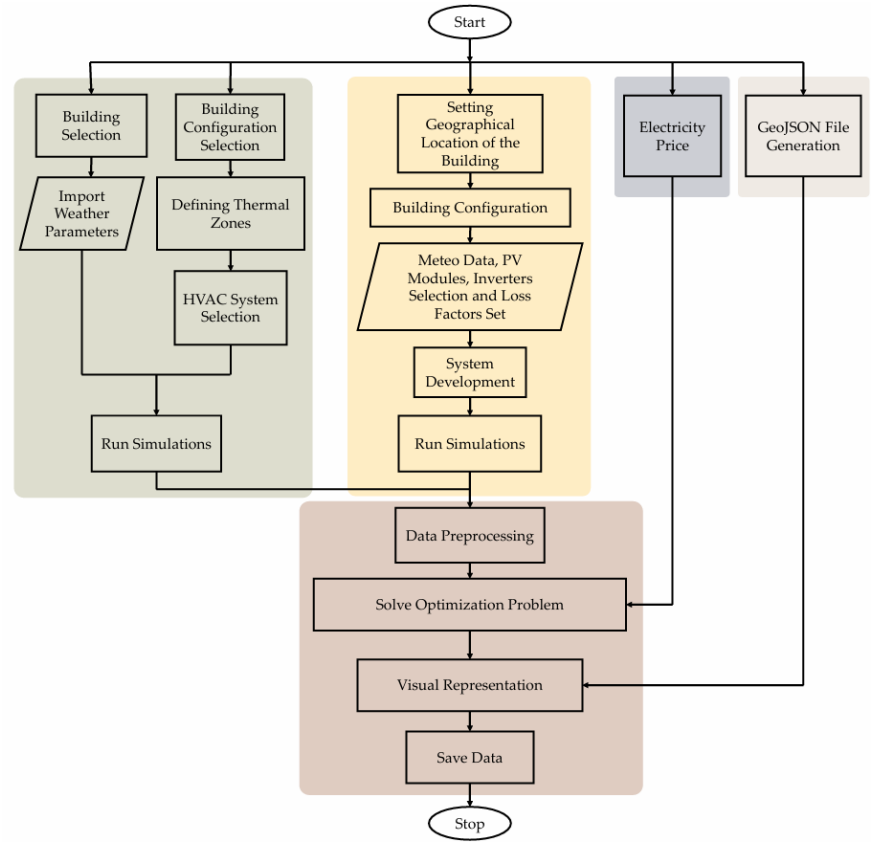

Figure 2

The flowchart diagram of the presented scientific study where five main sequences of the word are represented: (i) simulation of electrical energy generated by BIPV DSSC (highlighted in yellow); (ii) simulation of office building electrical energy consumption (represented in green); (iii) electricity price determination (marked in blue); (iv) generating GeoJSON file; and (v) solving optimization problem. Furthermore, HVAC refers to the Heating, Ventilation, and Air Conditioning system.

The different sections of the flowchart, represented with distinguishable colors, are explained in great detail, including the input parameters selection, in the following subsections. Nevertheless, the GeoJSON file contributes to the data visualization by making the research results more comprehensive.

2.2.1 Simulation of Electrical Energy Generated by BIPV DSSC

To simulate the electrical energy generated by BIPV DSSC systems, the PV*SOL (version 2023 R4 and 2025 R6) simulation environment has been employed, which offers customization options such as selection of photovoltaic modules, inverters, and geographical and environmental conditions. In addition, 3D modeling is provided, which allows obstacles like trees and neighboring buildings. Since DSSC is unavailable in the database of PV*SOL, one experimentally validated DSSC and two hypothetical DSSC modules were considered based on the literature review. Table 1 represents the technical parameters used to estimate the generated electrical energy. Two higher-power DSSC modules (Hypothetic DSSC#1 and Hypothetic DSSC#2) have been generated by extrapolation approaches applying series/parallel cell wiring rules. The first task was to set the geographic location, then the building configuration, and the meteorological conditions. Furthermore, followed by defining the photovoltaic modules and inverters, system losses have been set. The PV*SOL database has been used for meteorological data, including temperature, sunshine duration, and radiation values. Additionally, the applied three-dimensional simulation allowed a detailed evaluation of the building's structures, architectural elements, and ensured precise results by taking the surroundings of the OBs into consideration. The ground reflection factor, also known as albedo, was set to 20% and the annual performance loss due to dust accumulation was considered as 3% [23]. For system design, DSSC modules were integrated into the vertical facades of the OBs. One of the advantages of the use of DSSC is its ability to perform light harvesting efficiency under diffuse light conditions, which is remarkable compared to conventional silicon-based modules. In case of inverter selection, an "example" inverter configuration has been defined within the software, leaving the study independent of specific manufacturers. Beyond this, the designed system was an on-grid system.

Table 1
Technical parameters used to estimate the generated electric energy from the DSSC

Parameter	Real DSSC	Ref.	Hyp. DSSC #1	Ref.	Hyp. DSSC #2	Ref.	Dim.
Maximum Power Point Voltage	3.405	[24]	23.9	[25]	32.554	[26]	V
Maximum Power Point Current	0.707	[24]	3.336	[25]	3.2	[26]	A
Open-Circuit Voltage (V_{OC})	4.55	[24]	30.2	[25]	40.71	[26]	V
Short-Circuit Current (I_{SC})	0.945	[24]	3.665	[25]	3.61	[26]	A

Nominal Output	2.41	[24]	79.7	[25]	104.2	[26]	W
Fill Factor	56	[24]	72	[25]	72.9	[26]	%
Efficiency	4.6	[24]	11.1	[25]	14.5	[26]	%

After the simulation, data was collected and preprocessed. It can be concluded that while an increased number of walls can provide greater surface area for BIPV installation, the correlation is not linear. The number of simulations that were conducted was more than 400.

2.2.2 Simulation of Office Building Electrical Energy Consumption

To simulate the energy consumption of OB, the OpenStudio (OS) (version 3.5.1) integrated toolset has been utilized, which uses the EnergyPlus simulation engine. OS is a widely used tool for analyzing the energy efficiency of buildings. EnergyPlus meets the test criteria of American Society of Heating, Refrigerating and Air-Conditioning Engineers (ASHRAE) Standard 140/211 [23]. Various input data, including the geometry of the office building, its materials, meteorological parameters, location of the building, Heating, Ventilation, and Air Conditioning (HVAC) systems, were provided and set. The geometry of the buildings, incorporating floor plan, dimensions of windows, and the number of floors, is defined based on data from Google Earth Pro. In this regard, the floor plan concept was developed based on the study in [23]. In accordance with the aforementioned study, five interior spaces have been defined, which are (i) open office space (73%); (ii) corridor (16%); (iii) staircase (3%); (iv) kitchen (4%); and (v) restroom (4%). The percentage of each given interior space represents the proportion of each space in the total floor plan of each OB. Furthermore, the arrangement of interior spaces was set according to the methodology part of the Sorgato et al. study [23]. Variations in the placement of interior spaces have been examined, and the percentage change in the building's electricity consumption caused by the different arrangements has been determined. The results indicate that electricity consumption for heating fluctuated by 8%, and the energy for fan operation purposes fluctuated by 2.5%; however, the overall fluctuation of electricity consumption of the building was about 1%.

Additionally, the position of windows was the same for all the office buildings investigated. What's more, the distance from the floor to the lower edge of the windows was set to 1 meter, and the window-to-window ratio was equal to 0.4, which is a fixed value. The choice of the set parameters was based on Sorgato et al.'s work [23]. The built-in database was used for the material properties, thermal insulation, and other thermal characteristics of the element. The ASHRE 189.1-2009 standard gives guidelines for sustainable building construction to different climate zones [27]. According to the Köppen-Geiger climate classification, Budapest falls into a temperate climate zone, which corresponds to Climate Zone 4 in the ASHRAE standard [28]. Furthermore, lighting schedules, water consumption, and occupant movement parameters can be found in the OS database, and these

parameters are classified by climate zones. This available dataset has been used for the investigations.

Moreover, the HVAC system plays an important role in the indoor environment and comfort of the office building. The following criteria have been taken into consideration for selecting the HVAC system: (i) cooling processes should not rely on natural gas; and (ii) energy consumption should be minimized in the heating and cooling processes. Based on these considerations, the Packaged Rooftop Heat Pump (PRHP) HVAC system was chosen and used for all simulations. Constant parameters of the HVAC system were determined based on literature review as follows: Zone Air Distribution Effectiveness in Cooling Mode and Zone Air Distribution Effectiveness in Heating Mode were set to 1, and Minimum Zone Ventilation Efficiency was set to 0.8 [29]. It is notable that these uniformly used parameter values may not reflect the actual parameter values of each building, but the applied simulations provide an estimation of the building's monthly energy demand and help to understand the urgency of sustainable office buildings. Simulations have been carried out, and the generated data was collected.

2.2.3 Energy Price

Several scientific studies that deal with BIPV systems simplify their approach by applying a stationary electricity process in their models and calculations, making it easier to apply. In this regard, in the study of Sorgato et al., the electricity price was fixed tariff values, which were determined based on the Brazilian electricity provider for the investigated six cities [23]. Although accurate forecasting of time-dependent electricity prices is challenging due to a great deal of uncertainty factors. Among the various models, statistical techniques including autoregressive models (AR, ARMA, ARIMA) and multiple linear regression (MLR) and other hybrid methods are popular. Based on the work of Herczeg et al., the multivariate, particularly autoregressive, integrative, moving average (ARIMAX) method performs better during the energy crisis [30]. In the current study, two distinct approaches were taken into account: (i) fixed electricity price; and (ii) time-dependent electricity price.

(i) Fixed Electricity Price

For this scenario, official tariff data have been searched and collected from publicly available official websites of electricity suppliers. Table 2 shows the electricity tariffs in different cases under fixed prices analysis.

Table 2
Electricity tariffs in three different scenarios

	Scenarios	Electricity Price (Ft/kWh)
1	Flat Electricity Rate	37.751
2	Peak/Off-Peak Hour Tariff	Peak: 43.428; Off-Peak: 32.785
3	Heat Pump Version	23.539

Furthermore, peak and off-peak hour tariffs depend on the season: during wintertime, the peak hour tariff is between 6:00 and 22:00, while in summertime it is between 7:00 and 23:00. Consequently, the off-peak hour tariff is between 22:00 and 6:00 in wintertime and it is between 23:00 and 7:00 in summertime. The selling tariff was considered as 3 Ft/kWh based on the information on the official website of electricity suppliers.

(ii) Time-Dependent Electricity Price

Seasonal Autoregressive Integrated Moving Average with Exogenous Regressors (SARIMAX) model extends the classical ARIMA approach by taking the seasonality and exogenous regressors into account. Therefore, it is enabled to capture the complex dynamics in the time series, such as market conditions or weather fluctuations, in the case of electricity prices. McHugh et al. explored the use of SARIMAX for day-ahead forecasting for electricity prices. In their analysis, the results revealed that SARIMAX provides accurate forecasts with relatively low RMSE parameter [31]. The electricity price dataset was obtained from the EMBER database, which contains the electricity prices hourly for every European country. After the examination of the time series, gaps were identified, and to ensure continuity of the time series, the dataset was processed using linear interpolation to estimate intermediate values, and it was completed with the backward fill (also known as backfill) method to handle missing points at the end of the dataset. Exogenous regressors have been gathered based on reports about commodities such as coal – Newcastle, oil – Brent, natural gas, and carbon dioxide emission from the Investing.com webpage. The choice of exogenous regressors was guided by global commodity price indicators, which have a direct impact on electricity prices. Furthermore, these variables were included in the multivariate SARIMAX model to enhance the performance of the model. The electricity price data were available from 2015; however, the analysis period was restricted to data from 2019. The selection was based on the consideration that in the period following 2019, the energy sector witnessed considerable structural shifts due to geopolitical tensions, fuel price volatility, and other policies. Since the exogenous variable dataset was available on a daily resolution, the value duplication across time intervals method has been applied, which is a temporal unsampling approach to replicate uniform hourly time points. On the other hand, Herczeg et al. also investigated the dataset from 2019 [30]. Before applying forecast models, autocorrelation (ACF) and partial autocorrelation (PACF) diagnostics were performed to assess the relationship between current values and their past lags. These methods are crucial in the analysis of the appropriate lag structure for AR and MA terms. Based on the ACF plots, consistent spikes were dominant at regular 24-lags, reflecting a daily seasonality. Furthermore, PACF plots suggested a relatively short AR memory, resulting in a low-order seasonal AR term. In addition, stationarity of the time-dependent series was assessed using the Augmented Dickey-Fuller (ADF) test. The requirements for stationarity in the case of a time series are the following: (i) it has a constant mean; (ii) it has a constant variance; and (iii) its autocorrelation structure does not depend

on time. The null hypothesis (H_0) of the ADF states that the time series is non-stationary via the presence of a unit root. In this regard, the alternative hypothesis (H_1) suggests that it is stationary. The results of the Augmented Dickey-Fuller (ADF) test showed that the value of the test statistic is -6.864 with a critical value of -2.8616 at 5% significance level, associated with a small p-value of $1.5783 \cdot 10^{-9}$, which strongly supports the rejection of H_0, thereby providing statistical evidence in favor of H_1. This implies that the electricity price time series under investigation can be considered stationary according to the ADF test. In contrast, the exogenous parameters showed non-stationarity as determined by the same test. To assess the dynamic relationship between the target time series and exogenous variables, the Granger Causality (GC) test has been applied. In other words, to evaluate whether past values of exogenous variables (such as oil, natural gas, coal, and CO_2 prices) offer predictive power for target time series, the GC test was employed. For these purposes, first, each exogenous time series was transformed to achieve stationarity, which is required for the GC test. The results demonstrated at 5% significance level that statistically significant GC for most tested lags. These results indicate that the chosen exogenous parameters carry valuable information for modelling electrical energy time series. To further explore the underlying structure of the electricity price series, seasonal decomposition techniques have been employed using additive methods. The trend component revealed a long-term upward movement between mid-2021 and 2023. Additionally, regular and repeated fluctuations were observed at fixed intervals, indicating cyclical behavior. The residual component captured irregular variation. Guided by the insights obtained from partial autocorrelation, partial autocorrelation, Augmented Dickey Fuller test, Granger Causality and Seasonal Decomposition analysis – which revealed a non-stationary trend component –, Box-Jenkins methodology; literature-based model from the work of Herczeg et al. has been applied: SARIMAX(0, 0, 0)(1, 1, 0, 24) [30]. In order to conduct the analysis *Statsmodels* Python package has been used. To validate and compare the two applied SARIMAX models, a rolling-forecast procedure was implemented in a Python environment. The process utilized an iterative model training on an expanding time window. For each step prediction was made with a fixed horizon (one year ahead). As a next step, the training window was shifted forward by one day per iteration. For the evaluation, mean absolute error (MAE) and root mean squared error (RMSE) metrics have been used. Table 3 represents the applied metrics; their values, and their description used for time-dependent predictions.

Table 3

The applied evaluation metric and its description are used for time-dependent predictions

Metrics	Equation	Description	Model
MAE	$\frac{1}{n} \cdot \sum_{i=1}^{n} \lvert y_i - x_i \rvert$	The mean of absolute error between predictions and real values. The closer the value to zero, the more accurate the prediction	64.36

RMSE	$\sqrt{\frac{1}{n}\cdot\sum_{i=1}^{n}(x_i - y_i)^2}$	The root of the average magnitude of squared forecast errors. If it is closer to zero, the more accurate the model	105.77

To forecast realistic future driver energy prices using SARIMAX model, the exogenous parameters have been separately trained with XGBoost regression. The XGBoost method is a decision-tree-based gradient boosting algorithm in which each subsequent tree is trained to correct the residual errors left by its predecessors. Taking the regularization terms L1 and L2 into account, the model mitigates overfitting and delivers accurate regression models. The model was tuned via Bayesian hyperparameter search, resulting in a point forecast for all variables up to the end of the horizon. In order to quantify the uncertainty, a non-parametric Monte Carlo simulation has been added to the model, creating 1000 plausible paths for each driver supporting a 95% confidence interval. As a last step, these simulated exogenous variables were added to the pretrained and defined SARIMAX(0, 0, 0)(1, 1, 0, 24) model, and simulations were run. With realistic energy price trajectories, cost-minimization analysis with different scenarios can be investigated. To examine the scientific questions, in the next section, optimization techniques – the combination technique and genetic algorithms – have been applied using the previously simulated data and scenarios.

2.2.2 Optimization Solution

Finding the minimum value under given conditions is an essential mathematical discipline in optimization. Data was collected from simulations of electrical energy generated by BIPV DSSC, simulations of office building electrical energy consumption, and simulations of electrical energy prices (from time-series models). The processes were implemented in Python programming language using data manipulation and analysis packages (e.g., NumPy, Pandas). The core mathematical equations are defined as follows:

1. Set of Office Building Walls and Combination Sets

Let $W = \{w_1, w_2, \dots, w_n\}$ be a set of walls in each building which is covered by BIPV DSSC modules. The subset that contains k wall combinations can be defined as:

$$C_k(W) = \{c \subseteq W \mid |c| = k\} \quad (1)$$

The set $C_k(W)$ contains all possible subsets c that contain k elements.

2. Summation of Electrical Energy

Beyond that, each wall $w \in W$ has a time-dependent energy function given by $S_w(t)$ and the total energy generated over time (in other words, energy time series) for a given subset $c \in C_k(W)$. Equation (2) expresses the cumulative output energy for the selected set of walls.

$$E_c(t) = \sum_{w \in c} S_w(t) \quad (2)$$

3. Energy Difference Calculation

After the summation of electrical energy, energy differences have been calculated for a given combination c.

$$P_c(t) = E_c(t) - F(t) \tag{3}$$

Where: $F(t)$ represents the building's electricity consumption as a function of time.

4. Cost Calculation Based on Energy Difference

To evaluate the financial impact of the subsets, the conditional function has been determined as follows:

$$K_c(t) = \begin{cases} P_c(t) \cdot C_S(t), & if\ P_c(t) > 0, \\ P_c(t) \cdot C_b(t), & if\ P_c(t) < 0, \\ 0, & if\ P_c(t) = 0 \end{cases} \tag{4}$$

where $C_s(t)$ represents the selling price of electricity, and $C_b(t)$ represents the purchase price of electricity in function of time.

5. Selection of the Optimal Configuration

The summation of the cost calculation (total cost over time) helps to identify the optimal wall combination.

$$K_c = \sum_{t=1}^{N} K_c(t) \tag{5}$$

Consequently, the optimal configuration has been chosen based on equation (6), which indicates that wall configuration has the lowest positive total cost.

$$\min_{c \in \cup_{k=1}^{y} C_k(W)} \{K_c \mid K_c > 0\} \tag{6}$$

3 Results and Discussions

3.1 BIPV DSSC Energy Production versus the Building's Energy Demand

As a first step, the real DSSC module has been applied across all 34 office buildings for simulations. Data was collected and preprocessed for further investigations. Based on the analysis, it was revealed that the electricity generated by the real DSSC module could cover below 10% of each building's energy consumption or demand, even if a large façade area is installed. Furthermore, the net difference between energy produced by BIPV DSSC and the building's demand in every time step for each building was negative, so the applied system with the real DSSC never

produced surplus electrical energy. Consequently, equation (6) contributed negative values under all energy price scenarios. As a next step, hypothetical DSSC modules have been used for further investigations, but first, a building-selection procedure has been carried out to narrow the study to those buildings that might become suitable. Shading conditions, architectural geometry, and consumption magnitude have been jointly considered as selection criteria. Therefore, buildings with no prospect of positive return have been filtered out. The shading index (SI) has been introduced to capture and quantify the impact of neighboring buildings and surroundings. The shading index is the following: $SI = \sum_{k=1}^{N_b} \frac{H_k}{d_k^2} + \sum_{m=1}^{N_t} \frac{A_m}{d_m^2}$ where H_k is the height of the k-th neighboring building (m); d_k is the distance between façade and k-th building (m); A_m is radius of the m-th tree canopy; d_m is the distance between façade and m-th tree (m). Furthermore, SI < 0.45 (m^{-1}) as low-shading index was applied during the selection. As a result, ten office buildings were confined for hypothetical dye-sensitized solar cell analyses. The peak consumption of the chosen ten buildings never exceeded 275 kWh, and their shading indices were low. Figure 3 represents the three different types of DSSC module scenarios as their coverage ratio in a boxplot representation. The green boxplot shows the real DSSC, with orange color the hypothetical DSSC#1 can be seen, and blue color illustrates hypothetical DSSC#2. In the horizontal axis each month (from January to December) is shown, while in the vertical axis the coverage ratio in percentage representation can be indicated.

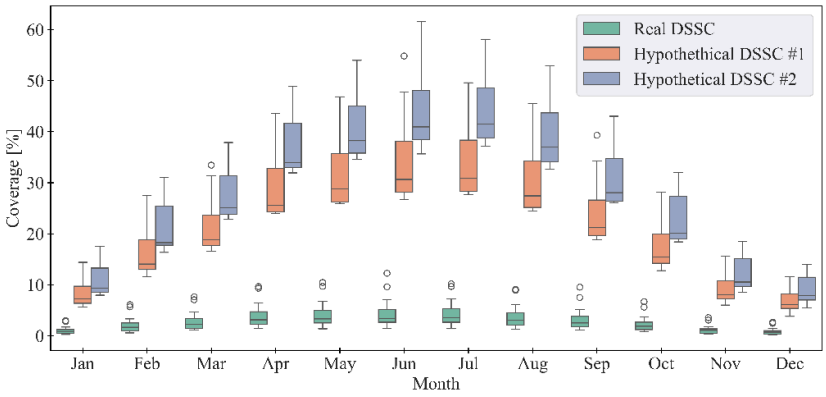

Distribution plot of BIPV DSSC system coverage in each month under three types of DSSC scenarios

From the figure, the following key insights can be drawn:

- The coverage is minimal in winter, especially in the case of the real DSSC, which remains around 2%. In contrast, the other types of DSSC scenarios rarely exceed 10-15% of coverage. Moderate coverage values can be investigated in spring and autumn seasons (in March-May, and in September-October months), where the median coverage is about 20-35%

for hypothetical DSSCs. For hypothetical #1, median is around 30-35% in summer, while for hypothetical #2 35-40% coverage %s is attained.

- Furthermore, hypothetical dye-sensitized solar cells show a promising option for BIPV systems, but they remain seasonal. On the other hand, while next-generation DSSC-based building-integrated photovoltaic modules can reduce the office buildings' energy deficit, these advanced technologies might not provide full-year coverage and remain seasonally driven.

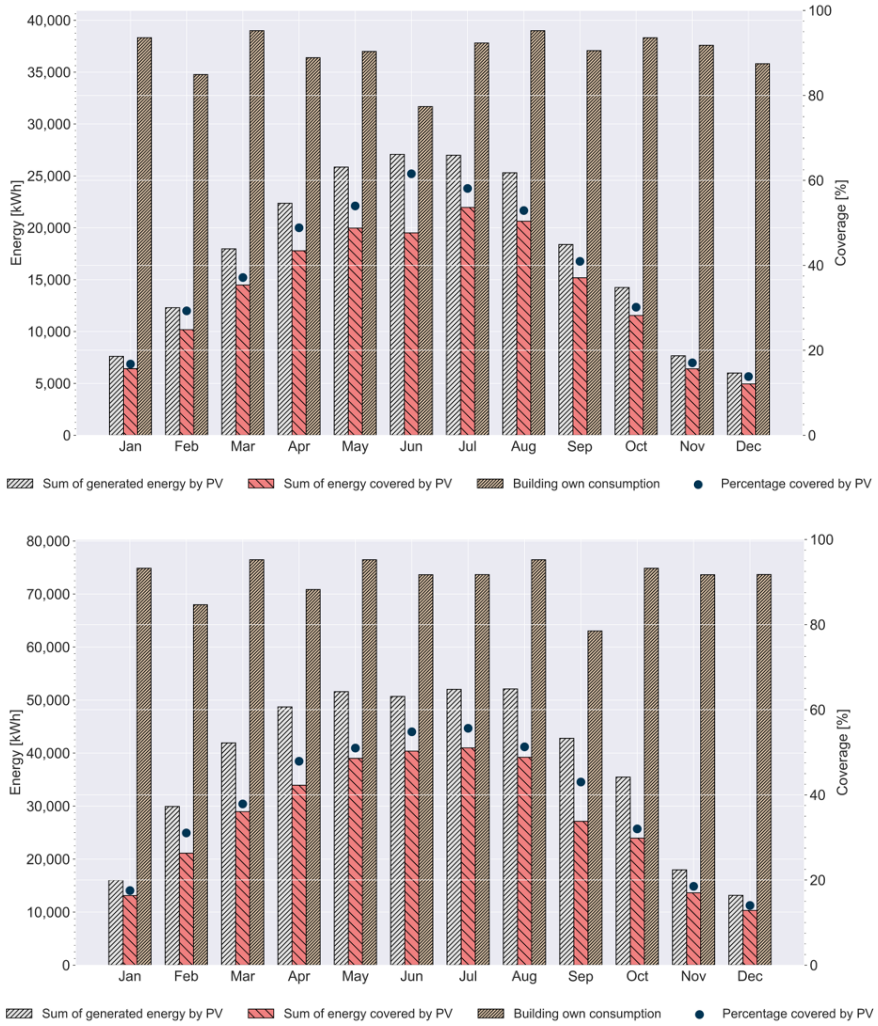

(b)

Figure 4

Monthly bar charts comparing the generated electrical energy by BIPV DSSC using hypothetical #2, the building's own demand in case of Building 1, shown in (a) and Building 2, shown in (b)

After reviewing the simulation of electrical energy generated by BIPV DSSC – using hypothetical #2 configuration – and the simulation of office building electrical energy consumption; two office buildings (Building 1 coordinates: (19.080460245120605, 47.52349944689746) and Building 2 coordinates: (19.05916100104892, 47.516111208487416)) have been selected for further investigation for which there are time steps when the generated electrical energy exceeds consumption. Although equation (6) remains negative for these cases. This selection was based on the consideration of fulfilling subpoint (ii.ii) of the scientific questions formulated above. In other words, these two buildings met the SI-consumption threshold and demonstrated at least one hour of positive net generation. Figure 4 represents the monthly totals for the BIPV DSSC system in the case of Building 1 and Building 2 using bar plot representation where the gray hatched bars illustrate the sum of energy generated by DSSC photovoltaic; coral hatched bars show the sum of electricity generation which covers the building's own consumption; brown hatched bars represent the building's own energy consumption. In connection with this, blue dots highlight the percentage coverage. Additionally, strong seasonality can be considered in each building, and the plots provide aggregated results with the previous boxplot shown.

3.2 Linear Programming Formulation

In this subchapter, the energy-price scenario was identified as providing a valid solution (in other words, a feasible solution) to Equation (6), enhancing the urban applicability of BIPV DSSC systems via supporting lower manufacturing costs. The objective function is formulated to determine the ratio between selling and buying prices in each building, see equation (7), where p_{sell} is the electricity selling price in Ft/kWh; p_{buy} is the electricity purchasing price, also in Ft/kWh; and ϕ is the minimum net revenue to be maximized. Equation (7) represents the objective function:

$$\max_{p_{sell},\ p_{buy},\ \phi} \quad \phi \tag{7}$$

subject to:

$$-\omega \cdot p_{sell} + \nu \cdot p_{buy} + \phi \leq 0 \tag{8}$$

$$p_{buy} \leq p_{sell} \tag{9}$$

$$\varepsilon \leq p_{sell} \leq p_{max} \tag{10}$$

$$r \cdot p_{max} \leq p_{buy} \leq p_{max} \tag{11}$$

where $\phi \geq 0$. In addition to this, for each time step (t) and each hypothetical DSSC scenario (j), the difference between generated electrical energy via BIPV DSSC and consumed electrical energy by the building $(\Delta E_{t,j})$ is calculated, and ω, ν aggregated parameters have been defined as:

$$\omega = \sum_j \sum_t \max(\Delta E_{t,j}, 0), \ \nu = \sum_j \sum_t \max(-\Delta E_{t,j}, 0) \quad (12)$$

After completing the simulations, data was saved and buy-ratio values were plotted by month and by season (as shown in Figure 5). Buy ratio values quantify the fraction of the selling price to the purchasing price. Considering Figure 5, the following conclusions can be drawn:

- Orange colorized bars represent buy-ration values belonging to Building 1 in each month; blue colorized bars illustrate the monthly optimal values in the case of Building 2; scatterplots show the seasonal maximum buy-ratio for each building.
- For Building 1, the buy-ratio values are significantly low in winter season and winter months – maximum peak is 8% - indicating that the BIPV DSSC system is feasible in winter months if the purchasing electricity price is no more than 8% of the selling price. Furthermore, significantly broader ranges occur from spring months (14% - 34%) to summer months (25% - 59%). The highest feasible peak appeals in June (59%), followed by May (34%) and July (31%). Consequently, spring and summer months are the most favorable months for BIPV DSSC system operation (37%). Although autumn (8%) and winter months (4%) have a low ratio, the system installation enhances the building's insulation.
- For the case of Building 2, a more consistent interval occurs in the late spring and summer months in the buy-ratio values. Based on the seasonal values, spring and summer are identical. What's more, the broadest window appears in September (43%), followed by April (40%). Comparing Building 2's monthly buy-ratio values with Building 1's monthly buy-ratio values, it can be seen that, except for May and June, higher monthly buy-ratio values occur in the case of Building 1.

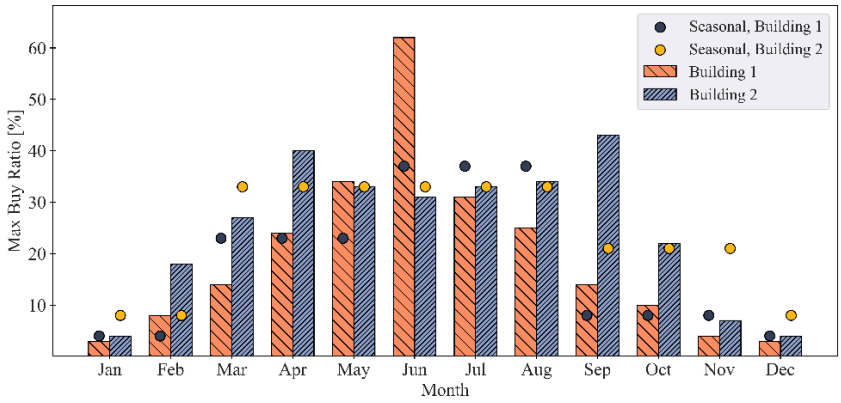

Maximum buy ratio value representation by month and by season for two office buildings, where the orange bar represents the values of Building 1 and the blue bar shows the values of Building 2. The dot illustrates the seasonal changes over the month.

Annual analysis has been conducted, and it is revealed that for Building 1, the annual buy ratio was 15%, whereas in the case of Building 2 this value reached 22%. Although monthly and seasonal fluctuations occur, the outcome supports decision-making in sustainability and green energy generation, helping the distribution of Dye-Sensitized Solar Cells in urban areas, thereby lowering the manufacturing cost of the device.

Conclusions

The number of office buildings in Budapest has been categorized, and simulations have been applied in function of time to determine the electrical energy production by the BIPV DSSC system, the building's own electrical energy demand and energy price scenarios. In addition to this, a comprehensive simulation framework has been developed and tested to enable the assessment of the performance of the BIPV DSSC system under real urban conditions. Moreover, in the current study, the applicability of BIPV DSSC systems has been evaluated using different dye-sensitized solar cell modules. Initially, a realistic DSSC module has been applied, and based on the results, it was revealed that these modules could cover below 10% of each building's energy demand, even if a large façade area is installed. Furthermore, the net difference between energy produced by BIPV DSSC and the building's demand in every time step for each building was negative, so the applied system with the real DSSC never produced surplus electrical energy. Thus, ten office buildings were used for hypothetical Dye-Sensitized Solar Cell analyses.

Based on these findings, the distribution of BIPV DSSC system coverage in each month under three types of DSSC scenarios has been investigated. From the observed results the following points have been deducted: (i) the coverage is minimal in winter, especially in the case of the reals DSSC which remains around 2%; (ii) the other types of DSSC scenarios rarely exceed 10-15% of coverage in winter seasons; (iii) Moderate coverage values were associated with spring and autumn seasons, while summer the median could reach the 40%. In addition to this, the energy-price scenario was identified to provide a valid solution for the optimization wall combination (equation (6)). From the observed results, it was revealed that the annualized buy ratio was 15% in the case of Building 1 and its' value reached 22%, in the case of Building #2.

Current energy-price scenarios demonstrate that the BIPV DSSC system is economically favorable. Conversely, by lowering the office building's electricity demand, the developed optimization approach can guide the selection of ideal facade sets.

Acknowledgements

The authors gratefully say thank you, for the support of the Obuda University, Doctoral School of Applied Informatics and Applied Mathematics. Supported by the 2024-2.1.1 University Research Scholarship Program of the Ministry for Culture and Innovation from the source of the National Research, Development and Innovation Fund.

References

[1] M. Malinowski, J. I. Leon, and H. Abu-Rub, 'Solar Photovoltaic and Thermal Energy Systems: Current Technology and Future Trends', Proc. IEEE, Vol. 105, No. 11, pp. 2132-2146, Nov. 2017, doi: 10.1109/JPROC.2017.2690343

[2] T. M. Pavlović, I. S. Radonjić, D. D. Milosavljević, and L. S. Pantić, 'A review of concentrating solar power plants in the world and their potential use in Serbia', Renewable and Sustainable Energy Reviews, Vol. 16, No. 6, pp. 3891-3902, Aug. 2012, doi: 10.1016/j.rser.2012.03.042

[3] J. Varga and Á. Csiszárik-Kocsir, 'The Impact of Human Activity on Environmental Elements Based on the Results of a Primary Research', ACTA POLYTECH HUNG, Vol. 21, No. 12, pp. 147-168, 2024, doi: 10.12700/aph.21.12.2024.12.9

[4] N. Martín-Chivelet, J. Polo, C. Sanz-Saiz, L. T. Núñez Benítez, M. Alonso-Abella, and J. Cuenca, 'Assessment of PV Module Temperature Models for Building-Integrated Photovoltaics (BIPV)', Sustainability, Vol. 14, No. 3, p. 1500, Jan. 2022, doi: 10.3390/su14031500

[5] A. A. M. Quran and R. Szabolcsi, 'Fuzzy Decision-Making for the Optimization of Off-Grid Multisource Power Generation Systems', ACTA POLYTECH HUNG, Vol. 22, No. 1, pp. 197-218, 2025, doi: 10.12700/aph.22.1.2025.1.11

[6] E. O. Yuzer and A. Bozkurt, 'Artificial Neural Network Models for Solar Radiation Estimation Based on Meteorological Data', ACTA POLYTECH HUNG, Vol. 22, No. 1, pp. 43-65, 2025, doi: 10.12700/aph.22.1.2025.1.3

[7] S.-H. Yoo, 'Optimization of a BIPV system to mitigate greenhouse gas and indoor environment', Solar Energy, Vol. 188, pp. 875-882, Aug. 2019, doi: 10.1016/j.solener.2019.06.055

[8] J. Sun and J. J. Jasieniak, 'Semi-transparent solar cells', J. Phys. D: Appl. Phys., Vol. 50, No. 9, p. 093001, Mar. 2017, doi: 10.1088/1361-6463/aa53d7

[9] H. M. Upadhyaya, S. Senthilarasu, M.-H. Hsu, and D. K. Kumar, 'Recent progress and the status of dye-sensitised solar cell (DSSC) technology with state-of-the-art conversion efficiencies', Solar Energy Materials and Solar Cells, Vol. 119, pp. 291-295, Dec. 2013, doi: 10.1016/j.solmat.2013.08.031

[10] B. O'Regan and M. Grätzel, 'A low-cost, high-efficiency solar cell based on dye-sensitized colloidal TiO2 films', Nature, Vol. 353, No. 6346, pp. 737-740, Oct. 1991, doi: 10.1038/353737a0

[11] A. Roy, A. Ghosh, S. Bhandari, P. Selvaraj, S. Sundaram, and T. K. Mallick, 'Color Comfort Evaluation of Dye-Sensitized Solar Cell (DSSC) Based Building-Integrated Photovoltaic (BIPV) Glazing after 2 Years of Ambient

Exposure', J. Phys. Chem. C, Vol. 123, No. 39, pp. 23834-23837, Oct. 2019, doi: 10.1021/acs.jpcc.9b05591

[12] A. K. Shukla, K. Sudhakar, P. Baredar, and R. Mamat, 'BIPV in Southeast Asian countries – opportunities and challenges', Renewable Energy Focus, Vol. 21, pp. 25-32, Oct. 2017, doi: 10.1016/j.ref.2017.07.001

[13] R. Corrao, D. D'Anna, M. Morini, and L. Pastore, 'DSSC-Integrated Glassblocks for the Construction of Sustainable Building Envelopes', AMR, Vol. 875-877, pp. 629-634, Feb. 2014, doi: 10.4028/www.scientific.net/AMR.875-877.629

[14] C. Cornaro et al., 'Comparative analysis of the outdoor performance of a dye solar cell mini-panel for building integrated photovoltaics applications: Comparative analysis of a dye solar cell mini-panel', Prog. Photovolt: Res. Appl., Vol. 23, No. 2, pp. 215-225, Feb. 2015, doi: 10.1002/pip.2426

[15] J. Y. Hyun, B. R. Park, N. H. Kim, and J. W. Moon, 'Building energy performance of DSSC BIPV windows in accordance with the lighting control methods and climate zones', Solar Energy, Vol. 244, pp. 279-288, Sep. 2022, doi: 10.1016/j.solener.2022.08.039

[16] T. Lund, W. A. Paskett, L. Højgård, and R. Neerup-Jensen, 'Performance and dye-stability of semi-transparent dye-sensitized solar cell pavilion modules after six years of operation', Journal of Physics and Chemistry of Solids, Vol. 179, p. 111396, Aug. 2023, doi: 10.1016/j.jpcs.2023.111396

[17] P. Kishore, N. Selvam, S. Didwania, and G. Augenbroe, 'Understanding BIPV performance with respect to WWR for energy efficient buildings', Energy Reports, Vol. 8, pp. 1073-1083, Nov. 2022, doi: 10.1016/j.egyr.2022.10.371

[18] H. Gholami and H. Nils Røstvik, 'The Effect of Climate on the Solar Radiation Components on Building Skins and Building Integrated Photovoltaics (BIPV) Materials', Energies, Vol. 14, No. 7, p. 1847, Mar. 2021, doi: 10.3390/en14071847

[19] A. Reale, L. Cinà, A. Malatesta, R. De Marco, T. M. Brown, and A. Di Carlo, 'Estimation of Energy Production of Dye-Sensitized Solar Cell Modules for Building-Integrated Photovoltaic Applications', Energy Technology, Vol. 2, No. 6, pp. 531-541, Jun. 2014, doi: 10.1002/ente.201402005

[20] J. B. Lee, J. W. Park, J. H. Yoon, N. C. Baek, D. K. Kim, and U. C. Shin, 'An empirical study of performance characteristics of BIPV (Building Integrated Photovoltaic) system for the realization of zero energy building', Energy, Vol. 66, pp. 25-34, Mar. 2014, doi: 10.1016/j.energy.2013.08.012

[21] S. Yang, A. Cannavale, A. Di Carlo, D. Prasad, A. Sproul, and F. Fiorito, 'Performance assessment of BIPV/T double-skin façade for various climate zones in Australia: Effects on energy consumption', Solar Energy, Vol. 199, pp. 377-399, Mar. 2020, doi: 10.1016/j.solener.2020.02.044

[22] J. Göndöcs, H. Breuer, R. Pongrácz, and J. Bartholy, 'Urban heat island mesoscale modelling study for the Budapest agglomeration area using the WRF model', Urban Climate, Vol. 21, pp. 66-86, Sep. 2017, doi: 10.1016/j.uclim.2017.05.005

[23] M. J. Sorgato, K. Schneider, and R. Rüther, 'Technical and economic evaluation of thin-film CdTe building-integrated photovoltaics (BIPV) replacing façade and rooftop materials in office buildings in a warm and sunny climate', Renewable Energy, Vol. 118, pp. 84-98, Apr. 2018, doi: 10.1016/j.renene.2017.10.091

[24] A. Hinsch et al., 'Dye solar modules for facade applications: Recent results from project ColorSol', Solar Energy Materials and Solar Cells, Vol. 93, No. 6-7, pp. 820-824, Jun. 2009, doi: 10.1016/j.solmat.2008.09.049

[25] Y. Chiba, A. Islam, Y. Watanabe, R. Komiya, N. Koide, and L. Han, 'Dye-Sensitized Solar Cells with Conversion Efficiency of 11.1%', jjap, Vol. 45, No. 7L, p. L638, Jul. 2006, doi: 10.1143/JJAP.45.L638

[26] J. Burschka et al., 'Sequential deposition as a route to high-performance perovskite-sensitized solar cells', Nature, Vol. 499, No. 7458, pp. 316-319, Jul. 2013, doi: 10.1038/nature12340

[27] N. Long, E. Bonnema, K. Field, and P. Torcellini, 'Evaluation of ANSI/ASHRAE/USGBC/IES Standard 189.1-2009', NREL/TP-550-47906, 984670, Jul. 2010. doi: 10.2172/984670

[28] L. Al-Ghussain, O. Al-Oran, and F. Lezsovits, 'Statistical estimation of hourly diffuse radiation intensity of Budapest City', Env Prog and Sustain Energy, Vol. 40, No. 1, p. e13464, Jan. 2021, doi: 10.1002/ep.13464

[29] C. Q. Li, 'Interpreting ASHRAE 62.1: ASHRAE Standard 62.1 is best known for its regulation of the amount of ventilation air delivered to each space in a commercial building by HVAC systems through various ventilation approaches to system design', Consulting Specifying Engineer, Vol. 56, No. 7, p. 35+, Aug. 2019

[30] B. Herczeg, Á. Csiszárik-Kocsir, and É. Pintér, 'Assessing the Accuracy of Electricity Price Forecasting Models, Before and After, the Impact of Energy Crisis Using Univariate and Multivariate Methods', ACTA POLYTECH HUNG, pp. 89-109, 2024, doi: 10.12700/aph.21.12.2024.12.6

[31] C. McHugh, S. Coleman, D. Kerr, and D. McGlynn, 'Forecasting Day-ahead Electricity Prices with A SARIMAX Model', in 2019 IEEE Symposium Series on Computational Intelligence (SSCI), Xiamen, China: IEEE, Dec. 2019, pp. 1523-1529. doi: 10.1109/SSCI44817.2019.9002930